Acute anti-inflammatory markers ITIH4 and AHSG in mice brain of a novel Alzheimer's disease model

Xiaowen Shi, Yasuyuki Ohta, Xia Liu, Jingwei Shang, Ryuta Morihara, Yumiko Nakano, Tian Feng, Yong Huang, Kota Sato, Mami Takemoto, Nozomi Hishikawa, Toru Yamashita and Koji Abe

Department of Neurology, Graduate School of Medicine, Dentistry and Pharmaceutical Sciences, Okayama University, 2-5-1 Shikatacho, Kitaku, Okayama 700-8558, Japan

Running headline: ITIH4 and AHSG expressions in Alzheimer's disease

Corresponding author: Prof. Koji Abe, Department of Neurology, Okayama University Graduate School of Medicine, Dentistry and Pharmaceutical Sciences, 2-5-1 Shikata-cho, Okayama 700-8558, Japan. Tel: +81-86-235-7365; Fax: +81-86-235-7368; E-mail: abekabek@cc.okayama-u.ac.jp

Abbreviations used: AD, Alzheimer's disease; Aβ, amyloid-β-peptide; ACs, ameroid constrictors; AHSG, alpha-2-HS-glycoprotein; BBB, blood-brain barrier; BCCAs, bilateral common carotid arteries; CTX, cerebral cortex; CBF, cerebral blood flow; DG, dentate gyrus; DAB, 3,3'-diaminobenzidine; HI, hippocampus; HP, hypoperfusion; ITIH4, inter-alpha-trypsin inhibitor heavy chain H4; IAIPs, inter-alpha inhibitor proteins; TH, thalamus.

Abstract

Alzheimer's disease (AD) is the most common dementia and a progressive neurodegenerative disorder aggravated by chronic hypoperfusion (HP). Since a lot of evidence suggest that inflammations are related with AD pathology, we investigated the expression change of two anti-inflammatory markers, inter-alpha-trypsin inhibitor heavy chain H4 (ITIH4) and alpha-2-HS-glycoprotein (AHSG), in a novel AD model (APP23) with HP at 12 month of age. As compared with wild type (WT, n=10), immunohistochemical analysis showed a higher ITIH4 and a lower AHSG expressions in the cerebral cortex, hippocampus, and thalamus of APP23 + HP group (n=12) than simple APP23 (n=10) group ($^*p < 0.05$ and $^{**}p < 0.01$ vs WT; $^{\#}p < 0.05$ and $^{\#\#}p < 0.01$ vs APP23). The present study provides an up-regulation of anti-inflammatory ITIH4 and a down-regulation of pro-inflammatory TNFα-dependent AHSG in a novel AD plus HP mice model.

Keywords: Alzheimer's disease, hypoperfusion, APP23 mice, inflammation, ITIH4, AHSG.

2

Introduction

Alzheimer's disease (AD) is the most common dementia accounting for 69% in elderly population more than 75 years old [1]. Cerebrovascular pathologies such as cerebral amyloid angiopathy, blood-brain barrier (BBB) disruption, and microvascular degeneration are confirmed in 60-90% of AD patients [2, 3]. A lot of studies show the involvement of the oxidative stress and neuroinflammatory processes in AD pathology [4-11].

Inter-alpha-trypsin inhibitor heavy chain H4 (ITIH4) is expressed in an acute phase of several pathological situations including infections and inflammations, and is associated with cell proliferation and migration [12]. Alpha-2-HS-glycoprotein (AHSG) is a novel anti-inflammatory hepatokine under acute injuries and infections, but is regulated by pro-inflammatory TNFα [13-15]. In recent years, ITIH4 and AHSG are reported as serum biomarkers in AD patient, but have not been fully investigated in AD brain [12, 16].

In the present study, therefore, we investigated the expression changes of ITIH4 and AHSG in the brain of novel AD model mice with chronic hypoperfusion (HP) to find the relation with AD pathology.

Materials and methods

Experimental model

The APP23 mouse model overexpresses human APP751 carrying the Swedish double

3

mutation (KM670/671NL) driven by a Thy1 promoter [17]. All animal experiments were performed in compliance with a protocol approved by the Animal Care and Use Committee of the Graduate School of Medicine and Dentistry of Okayama University (OKU-2014-095). This is a part of the whole project mainly focusing on inflammation in AD mice model. All used control mice were C57BL/6J. Animals were accommodated in 12/12 hours (h) light-dark cycle with a controlled temperature around 23°C and free access to food and water.

Three groups were designed in this study: wild type mice (WT + sham surgery, n=10), APP23 group (APP23 + sham surgery, n=10), and APP23 with chronic hypoperfusion (HP) group (APP23 + HP, n=12). Groups comprised approximately equal numbers of male and female mice.

Ameroid constrictors (ACs) with an inner diameter (D) of 0.75 mm (Research Instruments NW, Lebanon, OR, USA) were applied to induce chronic cerebral hypoperfusion. For the CCH group, a cervical incision was made and ACs were applied to bilateral common carotid arteries (BCCAs) at 4 months (M) of age. At the time points of 1, 3, 7, 14 and 28 d after surgery, a laser-Doppler flowmeter (FLO-C1, Omegawave, Tokyo, Japan) was used to measure cerebral blood flow (CBF) as our previous report (Zhai et al., 2016).

Tissue preparation

At 12M of age, mice were deeply anesthetized and then perfused with 20ml of ice-cold

phosphate-buffered saline (PBS, pH 7.4), followed by 20ml of ice-cold 4% paraformaldehyde (PFA) in 0.1 mol/L phosphate buffer. The brains were removed and post-fixed in the same fixation overnight at 4°C. After washing with PBS, the fixed tissues were transferred into 10, 20 and 30% (wt/vol) sucrose in PBS, each sucrose incubation step was for 24 h at 4°C. Then, the brains were frozen in dry ice and kept at -80°C. 20-μm thick coronal sections were prepared on a cryostat at -20°C and mounted on silane-coated glass slides.

Single immunohistochemistry analysis

For single immunohistochemistry, after incubation in 0.3% hydrogen peroxide/methanol for 30 min followed by 5% bovine serum albumin (BSA) in PBS with 0.1% triton for 1 h, the sections were stained overnight at 4°C with the following primary antibodies: rabbit anti-inter-alpha-trypsin inhibitor heavy chain H4 (ITIH4) antibody (1:50, Proteintech Group, Chicago, IL); rabbit anti-alpha-2-HS-glycoprotein (AHSG) antibody (1:50, Cloud-Clone Corp, Houston, TX, USA). After washed with PBS, brain sections were treated with suitable biotinylated secondary antibodies (1:500; Vector Laboratories, Burlingame, CA) for 2 h at room temperature. Then the sections were incubated with the avidin-biotin-peroxidase complex (Vectastain ABC Kit; Vector) for 30 min and visualized with 3, 3′-diaminobenzidine (DAB). Negative control sections were stained in the same manner as described above except for the primary antibodies.

Double immunofluorescence analysis

To analyze the localizations of ITIH4 and AHSG in neuronal cells, double immunofluorescent stainings for ITIH4 plus neuronal nuclear antigen (NeuN) and AHSG plus NeuN were performed. NeuN is used as a biomarker for neurons. Brain sections were incubated with 5% BSA in PBS for 1 h at room temperature. The following primary antibodies were used: rabbit anti-ITIH4 antibody (1:50, Proteintech Group, Chicago, IL); rabbit anti-AHSG antibody (1:50, Cloud-Clone Corp, Houston, TX, USA); mouse anti-NeuN antibody (1:200; Millipore, Burlington, MA). After rinsing in PBS, the sections were incubated with secondary antibodies conjugated to Alexa 488 and 555 (1:500, Molecular Probes, Eugene, OR) for 1 h at room temperature. The sections were then mounted using Vectashield mounting medium containing DAPI (Vector Laboratories, Burlingame, CA, USA), and scanned with a confocal microscope equipped with argon and HeNe1 laser (LSM-780; Zeiss, Jena, Germany).

Quantitative analysis

For each measurement, 3 sections per brain and 4 random selected regions were then analyzed with a light microscope (Olympus BX-51, Tokyo, Japan). The pixel intensity of ITIH4 and AHSG were measured at cerebral cortex (CTX), hippocampus (HI), and thalamus (TH) by an image processing software (Scion Image, Scion Corporation, Frederick, MD, USA).

Statistical analysis

All data are presented as mean ± SD. Statistical comparisons were performed using one-way analysis of variance based on a Tukey-Kramer post comparison. $p < 0.05$ was considered statistically significant.

Results

ITIH4 and AHSG expressions in CTX

Both ITIH4 and AHSG were obviously stained in neurons of CTX of WT mice (Fig. 1, top left). Although no significant difference of the pixel intensity of both ITIH4 and AHSG was detected between WT and APP23 group in the CTX, the pixel intensity of ITIH4 significantly increased in the APP23 + HP group as compared with the WT and APP23 group (Fig. 1, $^{**}p < 0.01$ vs WT; $^{#} p < 0.05$ vs APP23). In contrast, the pixel intensity of AHSG significantly decreased in the APP23 + HP group as compared with the WT group (Fig. 1, $^{*}p < 0.05$ vs WT).

ITIH4 and AHSG expressions in hippocampus (HI)

The ITIH4 was slightly stained in neurons of CA1, CA2 and CA3 (Fig. 2, top). Compared with the WT and APP23 group, the pixel intensity of ITIH4 significantly increased in the CA1, CA2 and CA3 of APP23 + HP group (Fig. 2, $^{*}p < 0.05$ and $^{**}p < 0.01$ vs WT; $^{#} p < 0.05$ and $^{##}$

7

$p < 0.01$ vs APP23). The AHSG was stained detected in the neurons of CA1, CA2 and CA3 of WT and APP23 mice (Fig. 3, top). While, the pixel intensity of AHSG significantly decreased in the CA1, CA2 and CA3 of APP23 + HP group compared with WT and APP23 group (Fig. 3, $^{**}p < 0.01$ vs WT; $^{##}p < 0.01$ vs APP23).

Both ITIH4 and AHSG were stained in the neurons of dentate gyrus (DG) (Fig. 4, top). Although no significant difference was observed in the pixel intensity of both ITIH4 and AHSG between WT and APP23 group, the pixel intensity of ITIH4 significantly increased in APP23 + HP group compared with WT and APP23 group (Fig. 4, $^{**}p < 0.01$ vs WT; $^{##}p < 0.01$ vs APP23). In contrast, the intensity of AHSG significantly decreased in APP23 + HP group compared with the WT and APP23 group (Fig. 4, $^{**}p < 0.01$ vs WT; $^{##}p < 0.01$ vs APP23).

ITIH4 and AHSG expression in TH

In the TH, the ITIH4 was scarcely detected in the neurons of WT mice (Fig. 5, top left), which was enhanced in both APP23 and APP23 + HP mice. Although no significant difference of the pixel intensity was detected between WT and APP23 group, the pixel intensity of ITIH4 significantly increased in the APP23 + HP group as compared with WT and APP23 mice (Fig. 5, $^{**}p < 0.01$ vs WT; $^{##}p < 0.01$ vs APP23). The AHSG was stained in the neurons of TH of WT mice. The pixel intensity of AHSG decreased in APP23 group compared with WT group, which was further emphasized in APP23 + HP group (Fig. 5, $^{*}p < 0.05$ and $^{**}p < 0.01$ vs WT;

[##] $p < 0.01$ vs APP23).

Localizations of ITIH4 and AHSG

Double immunofluorescence analysis showed that both ITIH4 and AHSG were expressed in neurons of both CTX and HI (Figs 6, 7), and mainly localized in the cytoplasm of neurons (Fig. 8).

Discussion

In the present study, we showed the up-regulated expression of ITIH4 and the down-regulation of AHSG in the neurons of CTX, HI, and TH of APP23 + HP mice model (Figs. 1-8).

ITIH4 belongs to the family of inter-alpha inhibitor proteins (IAIPs), which is expressed in a lot of tissues including liver, intestine, kidney, stomach, placenta and brain to signify their diverse biological functions by inhibiting serine proteases [13, 18-21]. ITIH4 is related to cell proliferation and migration during the development of the acute-phase inflammatory response and plays a role in the response for the inflammation of trauma and infection independent from pro-inflammatory TNFα [12, 22-24]. ITIH4 is a member of liver-derived ITI family having an anti-apoptotic and matrix-stabilizing functions. However, the role of ITIH4 has not been examined in cerebral ischemia or Alzheimer's disease. Therefore, we used a mouse model of

9

AD with HP to examine the pathological changes of ITIH4 in mice brain. Our previous studies showed that HP dramatically accelerated the progression of AD pathology accompanied with inflammation [25]. In addition, ITIH4 is regulated by IL-6, which regulates inflammation [26-28]. In the present study, HP significantly increased the expression of ITIH4 in the CTX, HI, and TH of APP23 mice (Figs. 1, 2, 4-8), suggesting that HP promoted the neuro-inflammation in the brains of AD model mice and ITIH4 may serve as a potential indicator of the progression of AD pathology.

In the response to injury and infection, the liver release many acute phase proteins including AHSG. AHSG is a cysteine protease inhibitor secreted from the liver to inhibit vascular calcification by preventing spontaneous mineral precipitation in the vasculature [29-31]. AHSG is regulated by several pro-inflammatory mediators [32], and produced as anti-inflammatory protein primarily in the liver under an acute inflammation phase[32]. However, AHSG is a negative acute phase reactant protein under the regulation of pro-inflammatory TNFα, attenuating inflammatory responses to injury and infection [13, 14]. In the present study, AHSG expression decreased in brains of APP23 + HP group (Fig. 1, 3, 4, 5), probably due to suppressions by pro-inflammatory TNFα, IL-1, and IL-6 [13, 14]. A previous paper showed the lower serum level of AHSG was related to the cognitive impairment in the mild-to-moderate AD patients accompanied by the higher concentration of TNF-α [16]. The decreased AHSG level may indicate the severity of AD progression in the present study (Figs. 1, 3, 4-8).

In summary, the present study demonstrated the expression changes of ITIH4 and AHSG in the brains of AD model mice accompanied by HP, suggesting the potential roles of ITIH4 and AHSG as candidate biomarkers to predict the severity of AD progression.

Conflict of interest

The authors disclose no potential conflict of interests.

References

[1]   Hishikawa N, Fukui Y, Sato K, Kono S, Yamashita T, Ohta Y, Deguchi K, Abe K (2016) Characteristic features of cognitive, affective and daily living functions of late-elderly dementia. *Geriatr Gerontol Int* **16**, 458-465.

[2]   Jellinger KA, Mitter-Ferstl E (2003) The impact of cerebrovascular lesions in Alzheimer disease--a comparative autopsy study. *J Neurol* **250**, 1050-1055.

[3]   Bell RD, Zlokovic BV (2009) Neurovascular mechanisms and blood-brain barrier disorder in Alzheimer's disease. *Acta Neuropathol* **118**, 103-113.

[4]   Akiyama H, Barger S, Barnum S, Bradt B, Bauer J, Cole GM, Cooper NR,

Eikelenboom P, Emmerling M, Fiebich BL, Finch CE, Frautschy S, Griffin WS, Hampel H, Hull M, Landreth G, Lue L, Mrak R, Mackenzie IR, McGeer PL, O'Banion MK, Pachter J, Pasinetti G, Plata-Salaman C, Rogers J, Rydel R, Shen Y, Streit W, Strohmeyer R, Tooyoma I, Van Muiswinkel FL, Veerhuis R, Walker D, Webster S, Wegrzyniak B, Wenk G, Wyss-Coray T (2000) Inflammation and Alzheimer's disease. *Neurobiol Aging* **21**, 383-421.

[5]   Schmidt R, Schmidt H, Curb JD, Masaki K, White LR, Launer LJ (2002) Early inflammation and dementia: a 25-year follow-up of the Honolulu-Asia Aging Study. *Ann Neurol* **52**, 168-174.

[6]   Engelhart MJ, Geerlings MI, Meijer J, Kiliaan A, Ruitenberg A, van Swieten JC, Stijnen T, Hofman A, Witteman JC, Breteler MM (2004) Inflammatory proteins in plasma and the risk of dementia: the rotterdam study. *Arch Neurol* **61**, 668-672.

[7]   Dik MG, Jonker C, Hack CE, Smit JH, Comijs HC, Eikelenboom P (2005) Serum inflammatory proteins and cognitive decline in older persons. *Neurology* **64**, 1371-1377.

[8]   Tan ZS, Beiser AS, Vasan RS, Roubenoff R, Dinarello CA, Harris TB, Benjamin EJ, Au R, Kiel DP, Wolf PA, Seshadri S (2007) Inflammatory markers and the risk of Alzheimer disease: the Framingham Study. *Neurology* **68**, 1902-1908.

[9]   Rojo LE, Fernandez JA, Maccioni AA, Jimenez JM, Maccioni RB (2008) Neuroinflammation: implications for the pathogenesis and molecular diagnosis of Alzheimer's disease. *Arch Med Res* **39**, 1-16.

[10]   Shang J, Yamashita T, Zhai Y, Nakano Y, Morihara R, Fukui Y, Hishikawa N, Ohta Y, Abe K (2016) Strong Impact of Chronic Cerebral Hypoperfusion on Neurovascular Unit, Cerebrovascular Remodeling, and Neurovascular Trophic Coupling in Alzheimer's Disease Model Mouse. *J Alzheimers Dis* **52**, 113-126.

[11]   Zhai Y, Yamashita T, Nakano Y, Sun Z, Shang J, Feng T, Morihara R, Fukui Y, Ohta Y, Hishikawa N, Abe K (2016) Chronic Cerebral Hypoperfusion Accelerates Alzheimer's Disease Pathology with Cerebrovascular Remodeling in a Novel Mouse Model. *J Alzheimers Dis* **53**, 893-905.

[12]   Yang MH, Yang YH, Lu CY, Jong SB, Chen LJ, Lin YF, Wu SJ, Chu PY, Chung TW, Tyan YC (2012) Activity-dependent neuroprotector homeobox protein: A candidate protein identified in serum as diagnostic biomarker for Alzheimer's disease. *J Proteomics* **75**, 3617-3629.

[13]   Daveau M, Jean L, Soury E, Olivier E, Masson S, Lyoumi S, Chan P, Hiron M, Lebreton JP, Husson A, Jegou S, Vaudry H, Salier JP (1998) Hepatic and extra-hepatic transcription of inter-alpha-inhibitor family genes under normal or acute inflammatory conditions in rat. *Arch Biochem Biophys* **350**, 315-323.

[14]   Li W, Zhu S, Li J, Huang Y, Zhou R, Fan X, Yang H, Gong X, Eissa NT, Jahnen-

Dechent W, Wang P, Tracey KJ, Sama AE, Wang H (2011) A hepatic protein, fetuin-A, occupies a protective role in lethal systemic inflammation. *PLoS One* **6**, e16945.

[15]   Mukhopadhyay S, Mondal SA, Kumar M, Dutta D (2014) Proinflammatory and antiinflammatory attributes of fetuin-a: a novel hepatokine modulating cardiovascular and glycemic outcomes in metabolic syndrome. *Endocr Pract* **20**, 1345-1351.

[16]   Smith ER, Nilforooshan R, Weaving G, Tabet N (2011) Plasma Fetuin-A is Associated with the Severity of Cognitive Impairment in Mild-to-Moderate Alzheimer's Disease. *Journal of Alzheimers Disease* **24**, 327-333.

[17]   Sturchler-Pierrat C, Abramowski D, Duke M, Wiederhold KH, Mistl C, Rothacher S, Ledermann B, Burki K, Frey P, Paganetti PA, Waridel C, Calhoun ME, Jucker M, Probst A, Staufenbiel M, Sommer B (1997) Two amyloid precursor protein transgenic mouse models with Alzheimer disease-like pathology. *Proc Natl Acad Sci U S A* **94**, 13287-13292.

[18]   Itoh H, Tomita M, Kobayashi T, Uchino H, Maruyama H, Nawa Y (1996) Expression of inter-alpha-trypsin inhibitor light chain (bikunin) in human pancreas. *J Biochem* **120**, 271-275.

[19]   Takano M, Mori Y, Shiraki H, Horie M, Okamoto H, Narahara M, Miyake M, Shikimi T (1999) Detection of bikunin mRNA in limited portions of rat brain. *Life Sci* **65**, 757-762.

[20]   Spasova MS, Sadowska GB, Threlkeld SW, Lim YP, Stonestreet BS (2014) Ontogeny of inter-alpha inhibitor proteins in ovine brain and somatic tissues. *Exp Biol Med (Maywood)* **239**, 724-736.

[21]   Xu H, Shang QH, Chen H, Du JP, Wen JY, Li G, Shi DZ, Chen KJ (2013) ITIH4: A New Potential Biomarker of "Toxin Syndrome" in Coronary Heart Disease Patient Identified with Proteomic Method. *Evidence-Based Complementary and Alternative Medicine*.

[22]   Pineiro M, Andres M, Iturralde M, Carmona S, Hirvonen J, Pyorala S, Heegaard PMH, Tjornehoj K, Lampreave F, Pineiro A, Alava MA (2004) ITIH4 (inter-alpha-trypsin inhibitor heavy chain 4) is a new acute-phase protein isolated from cattle during experimental infection. *Infection and Immunity* **72**, 3777-3782.

[23]   Bhanumathy CD, Tang Y, Monga SP, Katuri V, Cox JA, Mishra B, Mishra L (2002) Itih-4, a serine protease inhibitor regulated in interleukin-6-dependent liver formation: role in liver development and regeneration. *Dev Dyn* **223**, 59-69.

[24]   Yang MH, Yang YH, Lu CY, Jong SB, Chen LJ, Lin YF, Wu SJ, Chu PY, Chung TW, Tyan YC (2012) Activity-dependent neuroprotector homeobox protein: A candidate protein identified in serum as diagnostic biomarker for Alzheimer's disease. *Journal of Proteomics* **75**, 3617-3629.

[25]   Shang J, Yamashita T, Zhai Y, Nakano Y, Morihara R, Li X, Tian F, Liu X, Huang Y, Shi X, Sato K, Takemoto M, Hishikawa N, Ohta Y, Abe K (2018) Acceleration of NLRP3 inflammasome by chronic cerebral hypoperfusion in Alzheimer's disease model mouse. *Neurosci Res*.

[26]   Pineiro M, Alava MA, Gonzalez-Ramon N, Osada J, Lasierra P, Larrad L, Pineiro A, Lampreave F (1999) ITIH4 serum concentration increases during acute-phase processes in human patients and is up-regulated by interleukin-6 in hepatocarcinoma HepG2 cells. *Biochemical and Biophysical Research Communications* **263**, 224-229.

[27]   Li L, Choi BC, Ryoo JE, Song SJ, Pei CZ, Lee KY, Paek J, Baek KH (2018) Opposing roles of inter-alpha-trypsin inhibitor heavy chain 4 in recurrent pregnancy loss. *Ebiomedicine* **37**, 535-546.

[28]   Soler L, Dabrowski R, Garcia N, Alava MA, Lampreave F, Pineiro M, Wawron W, Szczubial M, Bochniarz M (2019) Acute-phase inter-alpha-trypsin inhibitor heavy chain 4 (ITIH4) levels in serum and milk of cows with subclinical mastitis caused by Streptococcus species and coagulase-negative Staphylococcus species. *Journal of Dairy Science* **102**, 539-546.

[29]   Ketteler M, Giachelli C (2006) Novel insights into vascular calcification. *Kidney International* **70**, S5-S9.

[30]   Jahnen-Dechent W, Heiss A, Schafer C, Ketteler M (2011) Fetuin-A regulation of calcified matrix metabolism. *Circ Res* **108**, 1494-1509.

[31]   Mori K, Emoto M, Inaba M (2011) Fetuin-A: a multifunctional protein. *Recent Pat Endocr Metab Immune Drug Discov* **5**, 124-146.

[32]   Wang H, Sama AE (2012) Anti-Inflammatory Role of Fetuin-A in Injury and Infection. *Current Molecular Medicine* **12**, 625-633.

Figure Legends

Fig. 1) Immunohistochemical stainings of ITIH4 and AHSG in the CTX of WT, APP23 and APP23 + HP groups (top), showing an increased pixel intensity of ITIH4 and a decreased pixel intensity of AHSG in APP23 + HP group ($^*p < 0.05$ and $^{**}p < 0.01$ vs WT; $^#p < 0.05$ vs APP23). Scale bar=50 μm.

Fig. 2) Immunohistochemical stainings of ITIH4 in the hippocampal CA1, CA2, and CA3 of WT, APP23 and APP23 + HP groups (top), showing increased pixel intensities in CA1, CA2, and CA3 of APP23 + HP group ($^*p < 0.05$ and $^{**}p < 0.01$ vs WT; $^#p < 0.05$ and $^{##}p < 0.01$ vs APP23). Scale bar=50 μm.

Fig. 3) Immunohistochemical stainings of AHSG in the hippocampal CA1, CA2, and CA3 of WT, APP23 and APP23 + HP groups (top), showing decreased pixel intensities in CA1, CA2, and CA3 of APP23 + HP group ($^{**}p < 0.01$ vs WT; $^{##}p < 0.01$ vs APP23). Scale bar=50 μm.

Fig. 4) Immunohistochemical stainings of ITIH4 and AHSG in the hippocampal DG of WT, APP23 and APP23 + HP groups (top), showing an increased pixel intensity of ITIH4 and a decreased pixel intensity of AHSG in APP23 + HP group ($^{**}p < 0.01$ vs WT; $^{##}p < 0.01$ vs APP23). Scale bar=50 μm.

Fig. 5) Immunohistochemical stainings of ITIH4 and AHSG in the TH of WT, APP23 and APP23 + HP groups (top), showing an increased pixel intensity of ITIH4 and a decreased pixel intensity of AHSG in APP23 + HP group ($^*p < 0.05$ and $^{**}p < 0.01$ vs WT; $^{##}p < 0.01$ vs APP23).

Scale bar=50 μm.

Fig. 6) Double immunofluoresecnt stainings of ITIH4 and NeuN in the CTX and HI of WT, APP23 and APP23 + HP groups, showing the localization of ITIH4 in neurons. Scale bar=50 μm.

Fig. 7) Double immunofluoresecnt stainings of AHSG and NeuN in the CTX and HI of WT, APP23 and APP23 + HP groups, showing the localization of AHSG in neurons. Scale bar=50 μm.
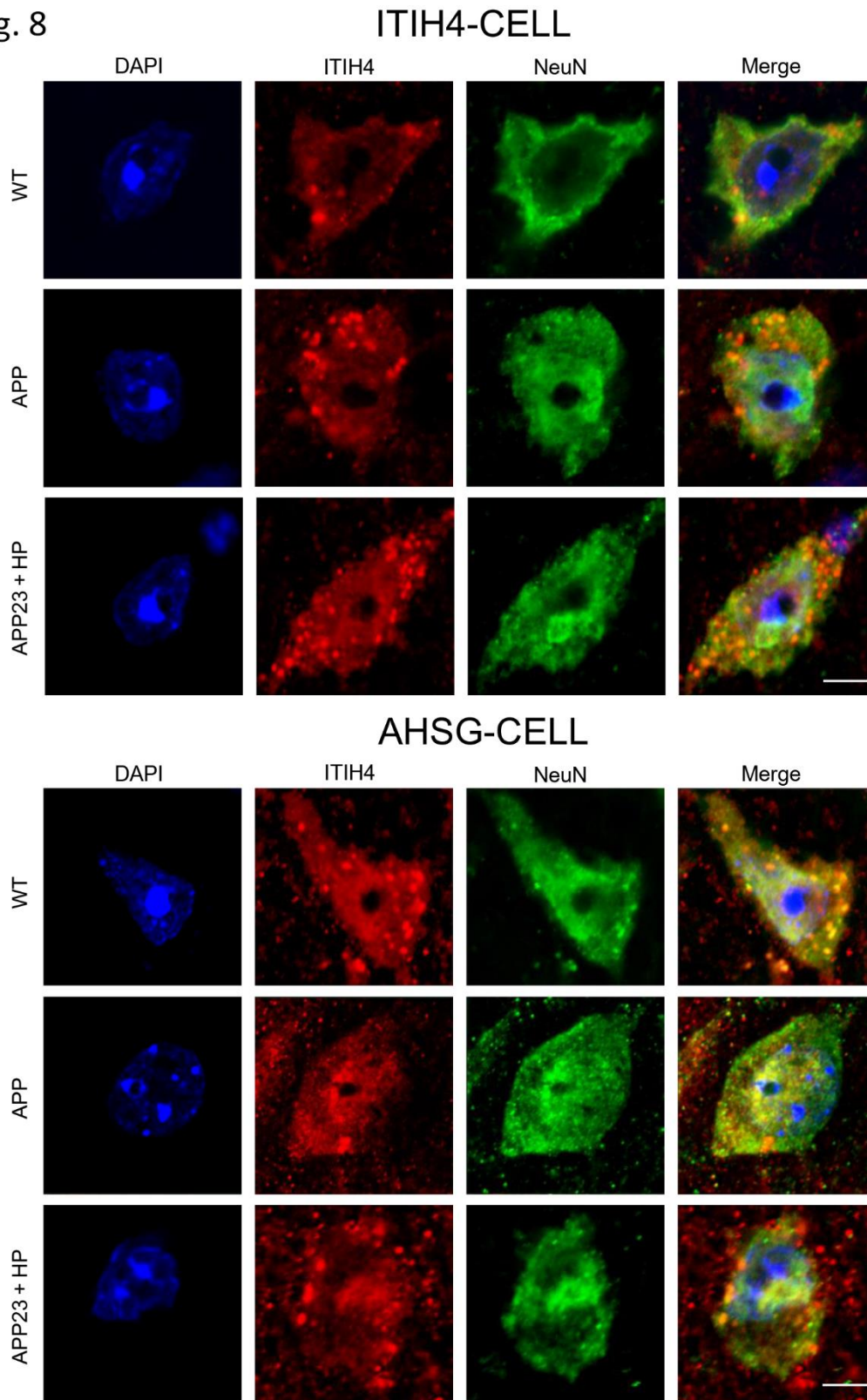
Fig. 8) Double immunofluoresecnt stainings of ITIH4 or AHSG plus NeuN in the CTX of WT,

APP23 and APP23 + HP groups, showing the main localizations of both markers in the

cytoplasm of neurons. Scale bar=20 μm.